Available online at www.sciencedirect.com
ScienceDirect
Physica B 403 (2008) 2241–2245
PHYSICA B
www.elsevier.com/locate/physb

Magnetic and magnetotransport properties of $La_{2/3}Ca_{1/3}MnO_3/Se_2FeMoO_6$ nano-crystalline composites synthesized under high pressure

L.D. Yao[a], P. E[a], J.S. Zhang[b], W. Zhang[a], F.Y. Li[a], C.Q. Jin[a], R.C. Yu[a,*]

[a]*Beijing National Laboratory for Condensed Matter Physics, Institute of Physics, Chinese Academy of Sciences, P.O. Box 603, Beijing 100080, PR China*
[b]*Department of Chemistry, Anyang Normal University, Anyang 455002, PR China*

Received 29 June 2007; received in revised form 29 November 2007; accepted 4 December 2007

Abstract

$La_{2/3}Ca_{1/3}MnO_3$ and Se_2FeMoO_6 nano-crystalline powders were pre-prepared using the polymer-network gel method, and the average grain sizes of $La_{2/3}Ca_{1/3}MnO_3$ and Se_2FeMoO_6 were about 40 and 50 nm, respectively. A series of $La_{2/3}Ca_{1/3}MnO_3/Se_2FeMoO_6$ nano-crystalline composites (molar ratio 1:1) were successfully synthesized under high pressure (4 GPa) and different treating temperatures. Due to the compositive influence of the smaller grain sizes, the Curie transition temperatures T_C (~225 K) for all composites are lower than that of the pure phase $La_{2/3}Ca_{1/3}MnO_3$. For the sample synthesized at the optimum conditions, the magnetoresistance value is close to 32% at 3 T and 5 K.

PACS: 81.07.−b; 72.80.Tm; 73.63.Bd; 75.47.Gk

Keywords: High pressure; Nano-crystalline composites; CMR

1. Introduction

Since the discovery of colossal magnetoresistance (CMR) effect [1–3] in manganese oxides with the perovskite structure $Ln_{1-x}A_xMnO_3$ (Ln: a rare-earth ion, A: an alkaline-earth cation), it has attracted great attention of scientists due to possible technological applications. The so-called CMR effect related to double exchange interaction is viewed as an intrinsic property of manganite materials. Typically, in the case of a single-crystal manganite, such as $La_{2/3}Ca_{1/3}MnO_3$(LCMO), the fall in resistance appears at or near the Curie temperature (T_C) under the effect of an external magnetic field [4,5]. However, since the CMR effect of manganites is restricted to a narrow range of temperature near the T_C and needs a large external magnetic field, it is difficult to apply them to electronic devices. Many experimentalists and theoreticians have been making great efforts in trying to improve the physical properties of the manganites for potential industrial uses. In 1996 Hwang et al. [6] reported another type of magnetoresistance (MR), intergranular MR in polycrystalline $La_{2/3}Sr_{1/3}MnO_3$. The MR, as an extrinsic effect, is related to spin-polarized tunneling through the insulating grain boundaries and is sensitive to low magnetic fields. Later, some polycrystalline or granular MR materials [7–11] with nano-metric scale were synthesized in order to increase the grain boundaries effect, and a larger MR value was reached in a low magnetic field.

As is well known, the low-field spin-polarized intergrain tunneling magnetoresistance (IMR) had also been observed in the double perovskite compound Sr_2FeMoO_6 (SFMO), which shows a high Curie temperature of 410–450 K and a large MR value at room temperature [12,13]. In some previous works on SFMO [14–17], it is proved that it is very effective to enhance the low-field IMR at room

*Corresponding author. Tel.: +86 10 82649159; fax: +86 10 82649531.
E-mail address: rcyu@aphy.iphy.ac.cn (R.C. Yu).

0921-4526/$ - see front matter © 2007 Elsevier B.V. All rights reserved.
doi:10.1016/j.physb.2007.12.003

temperature by reducing the size of the crystalline grains, indicating that the IMR is closely related to the grain boundaries.

Clearly, the grain boundary effect is a very significant factor to yield a high LFMR value in those materials. Besides the naturally formed grain boundaries existing in the single-phase granular materials, artificial grain boundaries [15,18] can also be added by making CMR/insulator composites, such as $La_{0.7}Sr_{0.3}MnO_3$/glass composites [19], LCMO/$SrTiO_3$ composites [20], LCMO/alumina composites [21], epitaxial LCMO/MgO nano-composite films, etc. It was observed that there is an enhancement in LFMR. Recently, CMR/CMR composites, such as SFMO homocomposites [22], were synthesized for controlling the magnetic and magnetotransport properties. In this paper, we introduce an effective experimental route, high-pressure composite way, to prepare LCMO/SFMO nano-crystalline composites and present some results on the physical properties of the composites.

2. Experimental

Nano-crystalline LCMO powder with an average grain size of 40 nm was first prepared by a polymer-network gel method [23–25] followed by heat treatment. According to the formula $La_{2/3}Ca_{1/3}MnO_3$, stoichiometric amounts of $La(NO_3)_3 \cdot 6H_2O$, $Ca(NO_3)_2 \cdot 4H_2O$ and $Mn(CHCOO)_2 \cdot 4H_2O$ were dissolved in deionized water containing citric acid, forming a uniform solution. After the pH value was regulated with ammonia, polymerization agents and starters were added to the solution. Being kept at a temperature of 80 °C for a few minutes, the solution polymerized into polymer gel. The gel was crushed, dried at 120 °C, and then fired at 500 °C in an oxygen atmosphere to convert the gel into LCMO superfine powder. The preparation process of nano-crystalline SFMO powder is similar to that of LCMO. In our experiments, $Fe(NO_3)_3 \cdot 9H_2O$, $Sr(NO_3)_2$ and $(NH_4)_6Mo_7O_{24} \cdot 4H_2O$ were used as raw materials. According to the approach mentioned above, superfine powders including SFMO were prepared. Finally, the powders were pelletized, heated at 700 °C for 6 h in a mixed gas stream of 1% H_2/Ar and then naturally cooled down in situ to room temperature to yield pure phase SFMO powders with an average grain size of 50 nm. In order to prepare LCMO/SFMO composites, the pre-prepared LCMO and SFMO powders were mixed with 1:1 molar ratio and then treated, respectively, at 25, 200, 400 and 600 °C under the same pressure of 4.0 GPa for 10 min.

The crystal structure and phase purity of the composites were examined by X-ray powder diffraction (XRD) with CuKα radiation at ambient temperature. The morphology of LCMO and SFMO were checked with an XL30 S-FEG scanning electron microscope (SEM). Magnetic and electrical properties of the composites were measured with Mag Lab Exa measurement system. The resistivity was measured as a function of temperature using a standard four points technique.

3. Results and discussion

The polymer-network gel method is a good way to prepare highly pure and superfine powders. The SEM images of the pre-prepared LCMO and SFMO powders are shown in Fig. 1, where it can be seen clearly that the particles are uniform and fine in the whole region. Moreover, the average grain sizes of the LCMO and SFMO powders are 30 and 40 nm, respectively. The chemical composition of the samples has been checked by energy dispersive X-ray microanalysis in situ in a SEM and determined to be close to the nominal compositions of the LCMO and SFMO.

According to the analyses of XRD patterns for the pure LCMO and SFMO samples, each of them shows a pure single phase without any detectable impurity. As is shown in Fig. 2, the diffraction peaks can be indexed in an orthorhombic structure (S. G.: Pbnm) and a tetragonal structure (S. G.: I4/mmm), respectively, for the LCMO and SFMO, which are in agreement with the relevant reports [10,26]. The XRD patterns of the composites prepared under different conditions are also displayed in Fig. 2, where it is observed that the diffraction peaks of an

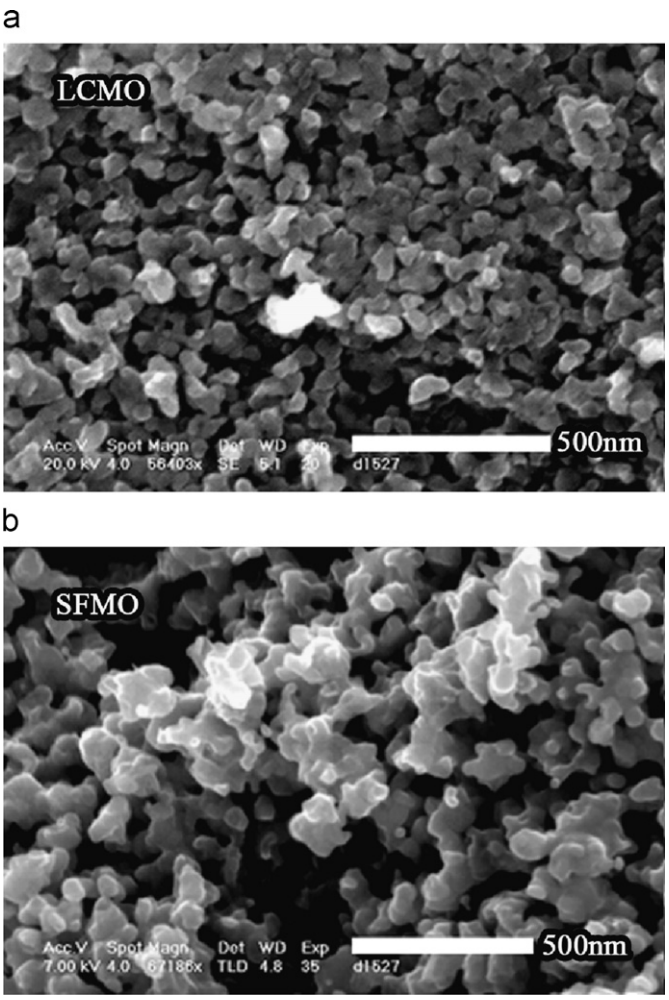

Fig. 1. SEM images of LCMO (a) and SFMO (b) powders.

impurity phase of $SrMoO_4$ gradually appear near 27° with the increase of treating temperature and the intensities become stronger as the treating temperature is more than 200 °C. The appearance of the impurity phase $SrMoO_4$ is considered to result from the oxidation reaction under high pressure. However, the grain sizes of the composites do not grow obviously through the analyses of full-width at half-maximum (FWHM) for the XRD diffraction peaks according to the Scherrer formula $d \approx \kappa\lambda/\beta\cos\theta$.

The general behavior of magnetization versus temperature indicates a long-range ferromagnetism below T_C for all composites, and the T_C remains unchanged around 225 K, as shown in Fig. 3. Since the smaller grains have larger surfaces and interfaces in the samples, the transition range becomes broader. Obviously, the Curie transition temperatures T_C (~225 K) for all the composites are less than that of pure LCMO. According to the previous reports [6,21], the most plausible explanation for the reduced transition temperature may result from the small grain size of the sample and microstructural inhomogeneities of oxygen distribution between and/or inside the grains. A reduction of grain size enhances the surface to volume ratio and leads to higher structural disorder within a surface layer, which in turn suppresses the magnetic exchange interaction. Thus the nano-crystalline manganites usually exhibit lower T_C as determined from magnetic measurements. Here, it should be noted that only the ferromagnetic transition of LCMO in all composites could be seen in the measuring temperature range. There seems not to be any clearly magnetic response coming from SFMO component in the composites. There might be two possible reasons for this phenomenon. One is, the grain boundaries in the composites can be viewed as paramagnetic boundaries. With the reduction of grain size, smaller FM domains separated by paramagnetic boundaries show weaker ferromagnetic coupling. The magnetization of SFMO might be more sensitive to the grain size than LCMO. Besides this, the impurity phase $SrMoO_4$ is a non-magnetic compound due to the empty 4d orbits in Mo^{6+} ion, so it results in the reduction of ferromagnetic coupling in the composites. The other is, the magnetic coupling between SFMO and LCMO grains might be complex in the nano-composites and cause the decrease of ferromagnetism of both components. But we believe there will be some indicative response in the magnetization around the ferromagnetic transition temperature of SFMO 410–450 K, which is out of our temperature measurement range.

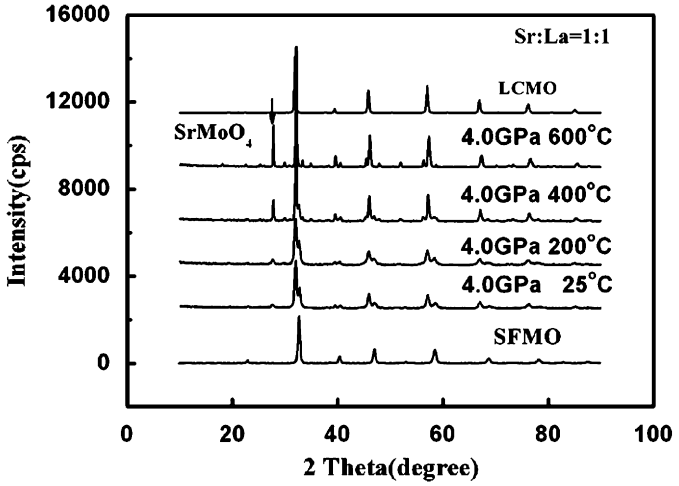

Fig. 2. Powder X-ray diffraction patterns of the LCMO/SFMO composites synthesized under different treating conditions.

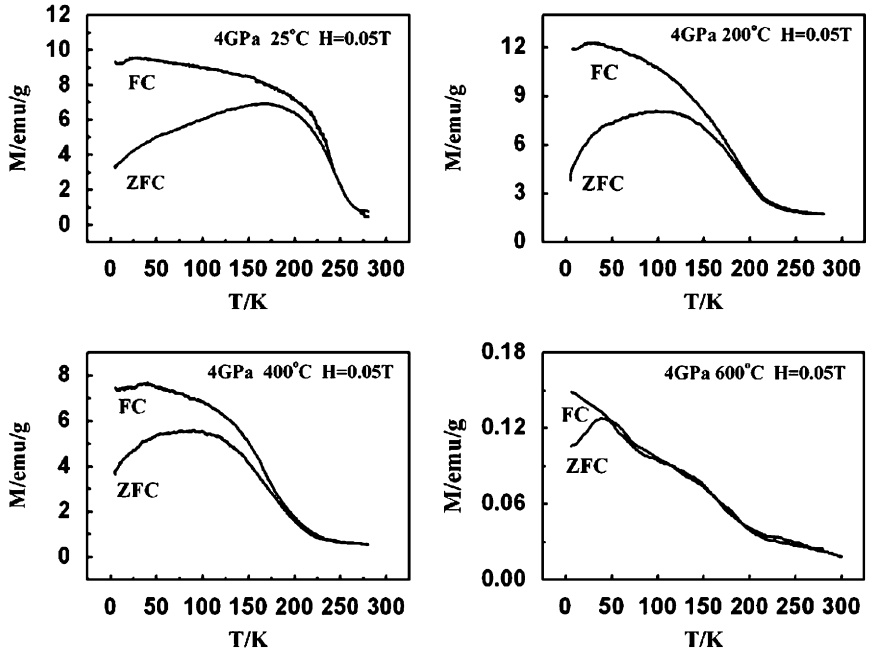

Fig. 3. Magnetization of the composites as a function of temperature after cooling in a zero magnetic field (ZFC) and in a field of 0.1 T (FC).

Moreover, at low temperature, the existence of spin-glass state was indicated by the measurement of the zero-field cooled and field cooled M–T curves in a magnetic field of 0.05 T. In Fig. 4 the hysteresis loops for all the composites show that the ferromagnetic ordering state exists at 5 K, and the magnetization tends to saturate under a low magnetic field. In addition, it can be seen that the saturation moments vary with different treating temperature. The saturation moment reaches a maximum for the sample treated at 200 °C and decreases with further increasing the treating temperature due to the occurrence of the $SrMoO_4$. According to the analyses of XRD and magnetic measurements mentioned above, the optimal treating conditions are determined as 4 GPa, 200 °C for 15 min. Herein , the sample synthesized at these conditions is defined as sample A.

The resistivities for the sample A were measured by the standard four-probe method in the temperature range of 5–300 K and in the magnetic fields up to 5 T. The resistivity versus temperature $R(T)$ curves measured at different magnetic fields are shown in Fig. 5, where the broad peaks in the R–T curves can be understood from a parallel resistor model since the sample A consists of parallel network of the conducting (LCMO and SFMO) and insulating (grain boundaries and $SrMoO_4$ insulator) paths. Especially, the impurity phase $SrMoO_4$ with an insulative behavior plays a negative role in the electron transport. Though the intergrain contribution is supposed to be reduced by high-pressure treatment, the resistivity curves still resemble the LCMO/insulator composites rather than mixing two metallic materials, such as the LCMO/CeO_2 nano-crystalline composites we reported in Ref. [27]. This shows again that the grain boundaries in the nanocomposites greatly affect the physical properties. According to the XRD analyses, the volume of the impurity phase $SrMoO_4$ occupies only a low ratio in the sample A, but it partially suppresses the metal–insulator transition. Because

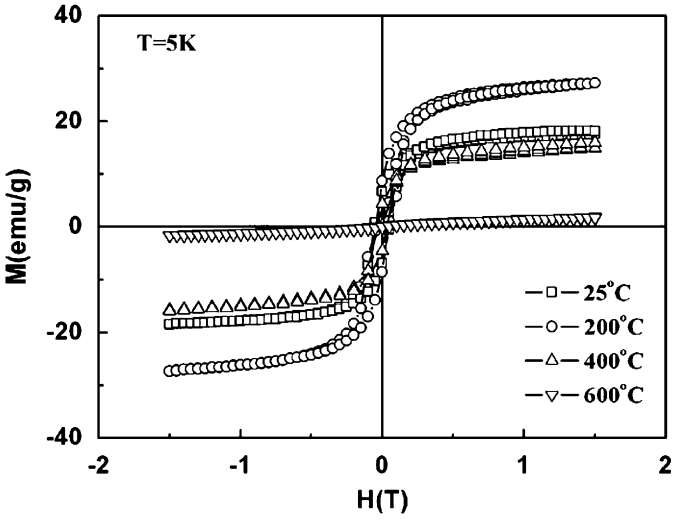

Fig. 4. Hysteresis loops of the LCMO/SFMO composites obtained at 5 K after cooling in a zero magnetic field.

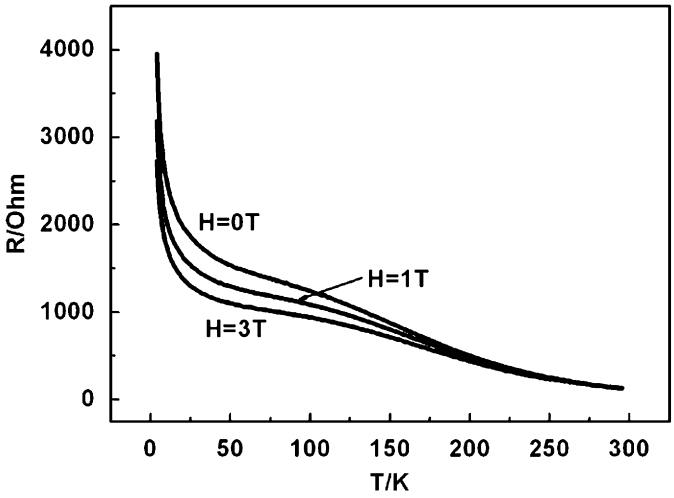

Fig. 5. The resistivity versus temperature $R(T)$ curves measured at different magnetic fields.

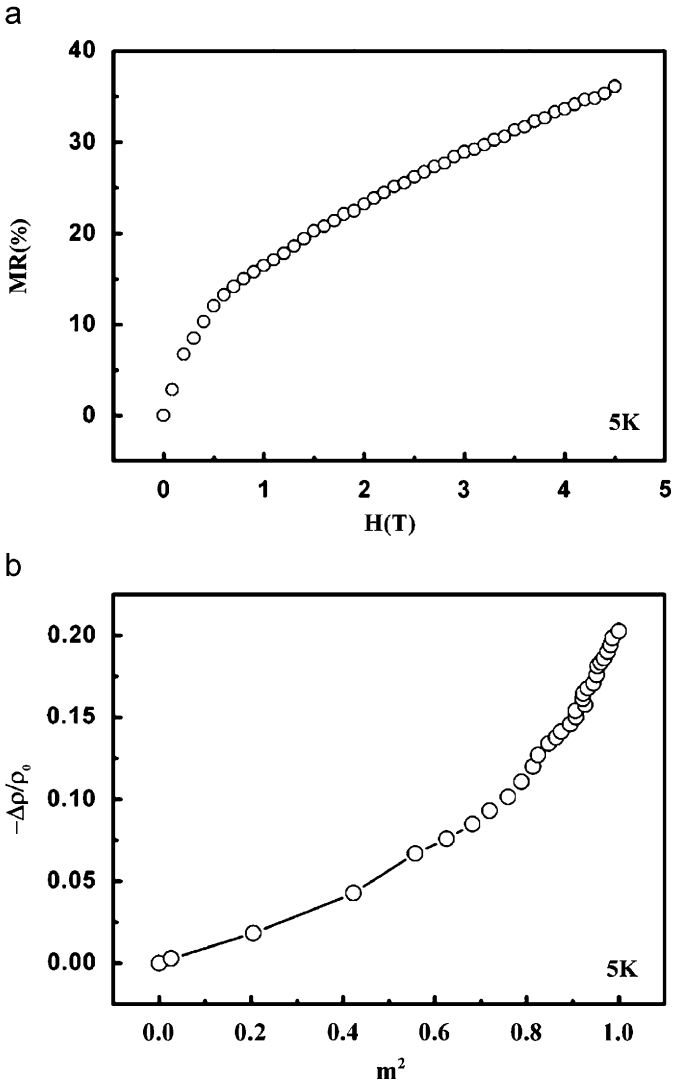

Fig. 6. (a) The field dependence of MR at 5 K for the sample A, (b) $-\Delta\rho/\rho(0)$ as a function of m^2 for the sample A.

it is difficult to overcome the barriers induced by insulating $SrMoO_4$ and grain boundaries for those conductive electrons with a lower kinetic energy at low temperatures, the resistivities increase rapidly below ~25 K. Moreover, with the increase of the external magnetic field, the obvious decrease in resistivity is observed below ~150 K, which indicates a large MR effect appearing at low temperatures. Here, the MR value is defined as: $-[\rho(H)-\rho(0)]/\rho(0)\times 100\%$. In Fig. 6(a), plots of the MR versus H are shown for the sample A at 5 K, where two distinguishable regions are exhibited in the field dependence of MR. That is, with increasing H, MR increases rapidly for $H<0.5$ T, but moderately and linearly for $H>0.5$ T. It is calculated that the magnetoresistance value is close to 32% and 19% at 3 T and 1 T, respectively. The values are slightly higher than that of pure SFMO (~26% and ~18% at 3 T and 1 T) [12]. In order to further investigate the origin of the MR enhancement, $-\Delta\rho/\rho(0)=-[\rho(H)-\rho(0)]/\rho(0)$ as a function of m^2 ($m=M/M_s$, where M_s is the saturation magnetization) instead of H are plotted in Fig. 6(b). The m^2 values are taken from the magnetization measurements. It is seen that $-\Delta\rho/\rho(0)$ exhibits a linear relationship with m^2 in the low-field region, i.e. $-\Delta\rho/\rho(0)\propto m^2$. As M approaches M_s, i.e., m is close to 1, the relationship deviates from the linearity and can be expressed as: $-\Delta\rho/\rho(0)=\alpha m^2+\beta m^4$. According to the relevant reports [6,28,29], the linearity in terms of m^2 is attributed to the spin-polarized tunneling in the boundaries between magnetic domains, while the deviation from the linear dependence on m^2 may imply some higher-order correlations between next-neighbor or next-next-neighbor grains of various spin polarization.

4. Conclusion

In our experiments, we have successfully prepared nanocrystalline LCMO and SFMO powders by means of the polymer-network gel method. A series of LCMO/SFMO composites have been synthesized using the high-pressure method. Based on the analyses of the XRD patterns and magnetic measurements, the optimal composite conditions are determined as 4 GPa, 200 °C for 15 min. The Curie transition temperatures T_C (~225 K) for all the composites are lower than that of the pure phase $La_{2/3}Ca_{1/3}MnO_3$ due to the coupling influence between the smaller grains of the LCMO and SFMO, grain boundaries, and the existence of the impurity phase $SrMoO_4$. The MR value is close to 32% and 19% at 3 and 1 T, respectively, for the composite synthesized at the optimal conditions.

Acknowledgments

This work was supported by the National Natural Science Foundation of China (Grant nos. 50471053 and 50621061) and the State Key Development Program for Basic Research of China (Grant nos. 2005CB623602 and 2007CB925003).

References

[1] R.M. Kusters, J. Singleton, D.A. Keen, R. McGreevy, W. Hayes, Physica B 155 (1989) 362.
[2] R. von Helmolt, J. Wecker, B. Holzapfel, L. Schultz, K. Samwer, Phys. Rev. Lett. 71 (1993) 2331.
[3] K. Chahara, T. Ohno, M. Kasai, Y. Kozono, Appl. Phys. Lett. 63 (1993) 1990.
[4] A. Urushibara, Y. Moritomo, T. Arima, A. Asamitsu, G. Kido, Y. Tokura, Phys. Rev. B 51 (1995) 14103.
[5] J.Z. Liu, I.C. Chang, S. Irons, P. Klavins, R.N. Shelton, K. Song, S.R. Wasserman, Appl. Phys. Lett. 66 (1995) 3218.
[6] H.Y. Hwang, S.W. Cheong, N.P. Ong, B. Batlogg, Phys. Rev. Lett. 77 (1996) 2041.
[7] W.E. Picket, D.J. Singh, Phys. Rev. B 53 (1996) 1146.
[8] M. Ziese, Rep. Prog. Phys. 65 (2002) 143.
[9] J.H. Park, E. Vescovo, H.J. Kim, C. Kwon, R. Ramesh, T. Venkatesan, Nature (London) 392 (1998) 794.
[10] R.D. Sánchez, J. Rivas, C. Vázquez-Vázquez, A. López-Quintela, M.T. Causa, M. Tovar, S. Oseroff, Appl. Phys. Lett. 68 (1996) 134.
[11] L.E. Hueso, J. Rivas, F. Rivadulla, M.A. López-Quintela, J. Appl. Phys. 86 (1999) 3881.
[12] K.I. Kobayashi, T. Kimura, H. Sawada, K. Terakura, Y. Tokura, Nature 395 (1998) 667.
[13] T.H. Kim, M. Uehara, S.W. Cheong, S. Lee, Appl. Phys. Lett 74 (1999) 1737.
[14] K.L. Ju, J. Gopalakrishnan, J.I. Peng, Q. Li, G.C. Xiong, T.V. Venkatesan, R.G. Green, Phys. Rev. B 51 (1995) 6143.
[15] J.Z. Sun, W.J. Gallagher, P.R. Duncombe, L. Krusin-Elbaum, R.A. Altman, A. Gupta, Y. Lu, G.Q. Gong, G. Xiao, Appl. Phys. Lett. 69 (1996) 3266.
[16] H.Y. Hwang, S.W. Cheong, Nature 389 (1997) 942.
[17] H.Y. Hwang, S.W. Cheong, Science 278 (1997) 1607.
[18] C. Kwon, Q.X. Jia, Y. Fan, M.F. Hundley, D.W. Reagor, J.Y. Coulter, D.E. Peterson, Appl. Phys. Lett. 72 (1998) 486.
[19] S. Gupta, R. Ranjit, C. Mitra, P. Raychaudhuri, R. Pinto, Appl. Phys. Lett. 78 (2001) 362.
[20] D.K. Petrov, L. Krusin-Elbaum, J.Z. Sun, C. Field, P.R. Duncombe, Appl. Phys. Lett. 75 (1999) 995.
[21] L.E. Hueso, J. Rivas, F. Rivadulla, M.A. López-Quintela, J. Appl. Phys. 89 (2001) 1746.
[22] Y.H. Huang, J. Lindén, H. Yamauchi, M. Karppinen, Appl. Phys. Lett. 86 (2005) 072510.
[23] W.B. Yelon, Z. Hu, W.J. James, G.K. Marasinger, J. Appl. Phys. 79 (1996) 5939.
[24] H.W. Zhang, S.Y. Zhang, B.G. Shen, C. Lin, J. Appl. Phys. 85 (1999) 4660.
[25] J.H. Lin, S.F. Liu, X.L. Qian, M.Z. Su, J. Alloys Compds. 238 (1996) 113.
[26] P. E, J.S. Zhang, L.D. Yao, F.Y. Li, Z.X. Bao, J.X. Li, Y.C. Li, J. Liu, C.Q. Jin, R.C. Yu, J. Mater. Sci. 41 (2006) 7374.
[27] L.D. Yao, W. Zhang, J.S. Zhang, H. Yang, F.Y. Li, Z.X. Liu, C.Q. Jin, R.C. Yu, J. Appl. Phys. 101 (2007) 063905.
[28] J.Q. Xiao, J.S. Jiang, C.L. Chien, IEEE Trans. Magn. 29 (1993) 2688.
[29] J.S. Helman, B. Abeles, Phys. Rev. Lett. 37 (1976) 1429.